SUPPORTING INFORMATION

Direct observation of the cyclic dimer in liquid acetic acid by probing the C=O vibration with ultrafast coherent Raman spectroscopy

Matthias Lütgens, Frank Friedriszik, and Stefan Lochbrunner*

Institut für Physik, Universität Rostock, D-18055 Rostock, Germany, Email: stefan.lochbrunner@uni-rostock.de

1 Concentration dependent CARS and Raman spectra of acetic acid in carbon tetrachloride

Figure S1 shows the linear Raman and time and frequency resolved CARS spectra of neat AA and AA diluted in carbon tetrachloride. The Raman and CARS results of neat AA have to be interpreted assuming four contributions as discussed in the main article. In the binary mixtures of AA with CCl_4 the contributions of mode II and III are clearly reduced compared to mode I and the dephasing times tend to become longer (lower panels). Mode I, which dominates after the cross-correlation, originates from the cyclic dimer. In the sample with the lowest mole fraction of AA, beside of mode I, only small signatures of mode III are remaining, probably caused by monomers.

Figure S2 shows simulations of the CARS spectra. The parameters used in the reconstruction of the signal are summarized in Table S1. Modes with considerably slow dephasing can be analyzed in more detail and the corresponding parameters are printed in bold. With increasing content of CCl_4 a decreasing dephasing rate is observed which means in terms of line widths a narrowing in the diluted cases. In the last panel signatures from the solvent CCl_4 contribute significantly to the spectra. However, these modes dephase almost within the cross-correlation.

Extended Raman spectra of the AA/CCl_4 mixtures are shown in Fig. S3. Here, the CH_3 deformation mode at 1428 cm^{-1} is seen, which contributes with its wing also somewhat to the CARS signal during the cross correlation.

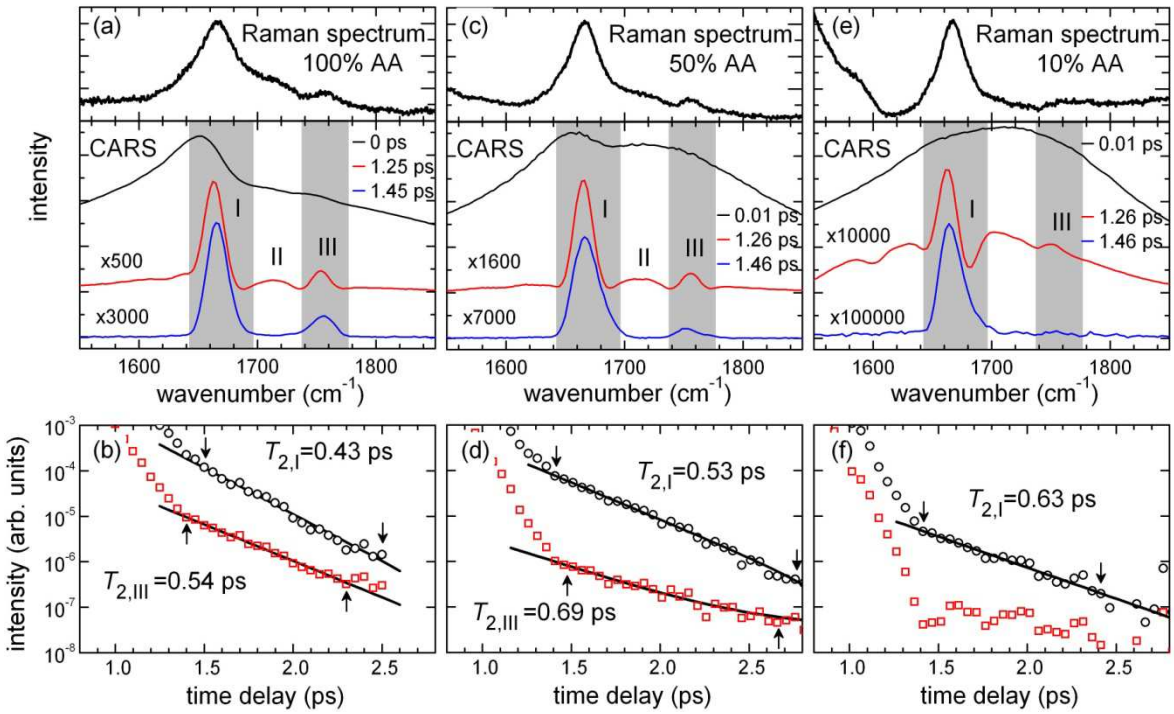

Fig. S1 (a) Raman and selected CARS spectra of 100vol% acetic acid, (b) frequency integrated and normalized time trace of modes I and III with mono exponential fits. The arrows indicate the data range selected for least square fitting. Panels (c)-(f) show the same for acetic acid diluted in carbon tetrachloride at different concentrations.

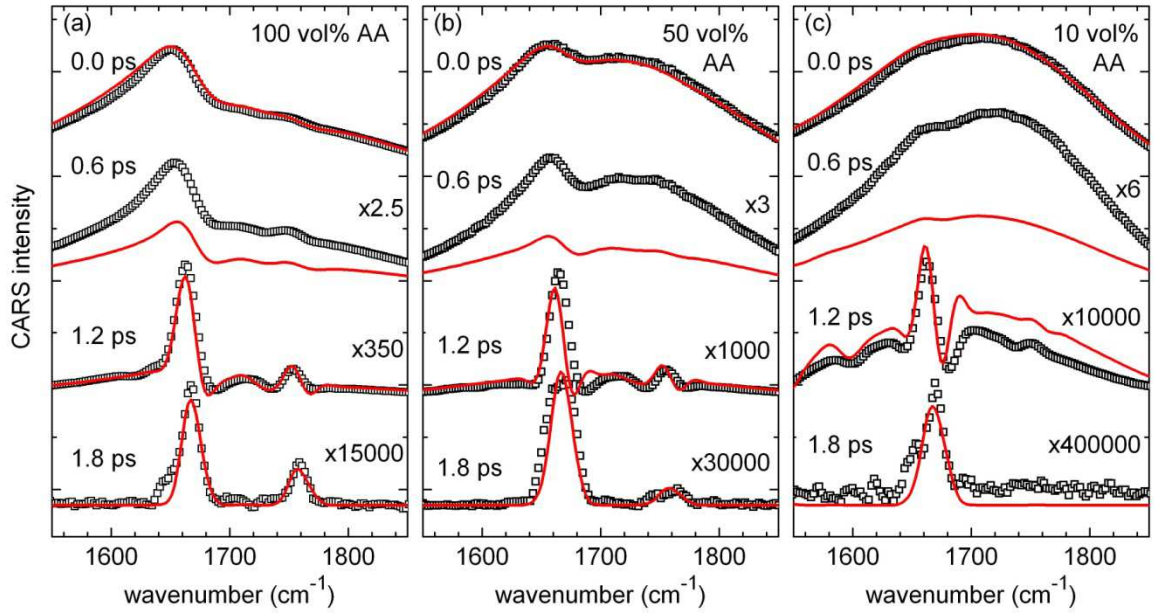

Fig. S2 Simulations of the CARS spectra of neat AA as well as of AA diluted in CCl_4.

Table S1 Simulation parameters for the investigated AA / CCl_4 mixtures. The values extracted from the analysis of the CARS spectra are printed in bold. The other parameters are highly uncertain due to low amplitudes and/or fast dephasing rates.

	100 vol% AA		50 vol% AA		10 vol% AA	
No.	ω_{vib} / cm^{-1}	$\delta\omega_{vib}$ / cm^{-1}	ω_{vib} / cm^{-1}	$\delta\omega_{vib}$ / cm^{-1}	ω_{vib} / cm^{-1}	$\delta\omega_{vib}$ / cm^{-1}
Ia	1669	53	1669	48	-	-
Ib	**1668**	**25**	**1667**	**20**	**1668**	**17**
II	1719	48	1719	48	-	-
III	**1759**	**20**	**1759**	**15**	1759	13
$\delta_a CH_3$	1428	48	-	-	-	-
CCl_4 I	-	-	-	-	1511	48
CCl_4 II	-	-	1528	70	1534	48
CCl_4 III	-	-	-	-	1588	46

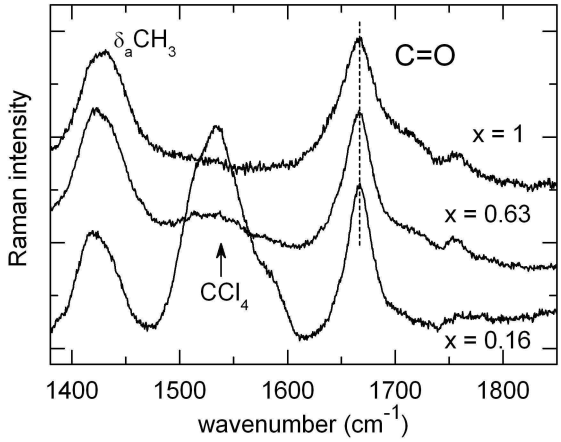

Fig. S3 Extended Raman spectra of AA/CCl_4 mixtures. The intensities are scaled with respect to the C=O mode at 1665 cm^{-1}

2 Polarisation resolved Raman spectra of neat acetic acid and conventional Raman spectra of neat deuterated AA derivates

Linear Raman spectra for parallel and perpendicular polarization with respect to the excitation polarization are shown in figure S4 (a). The intensity of the spectrum measured for perpendicular polarization is drastically reduced. Although the shape is a bit different, essentially the entire C=O vibrations cause a polarized signal, whether they are originating from the cyclic dimer, chain structure or any other possible structure. Especially, the main feature is reduced almost completely. This means it has to be totally symmetric, which is fulfilled for the C=O stretch vibrations in the cyclic dimer, linear chains and single AA molecules. All discussed structures are planar, and the Raman active vibration is an in-plane vibration in the chain like dimer as well as in the cyclic dimer. Therefore depolarization spectra allow in the case of the C=O band of AA no clear disentanglement of the contributions originating from different structural species.

The same applies to AA with deuterated hydroxyl or methyl groups as shown in Fig. S4 (b). The three separated contributions of neat AA are in principle found in the deuterated derivates, too. The shifts might be explained by differences in the effective masses involved in the vibrations and maybe by changes in the H-bond interactions. Depending on the geometry, the local motions of the deuterated side groups are involved to some extent in the normal coordinate displacements of the C=O stretch vibration. This causes different shifts to lower energies, but a clear separation into more than three contributions is not seen on the first glance.

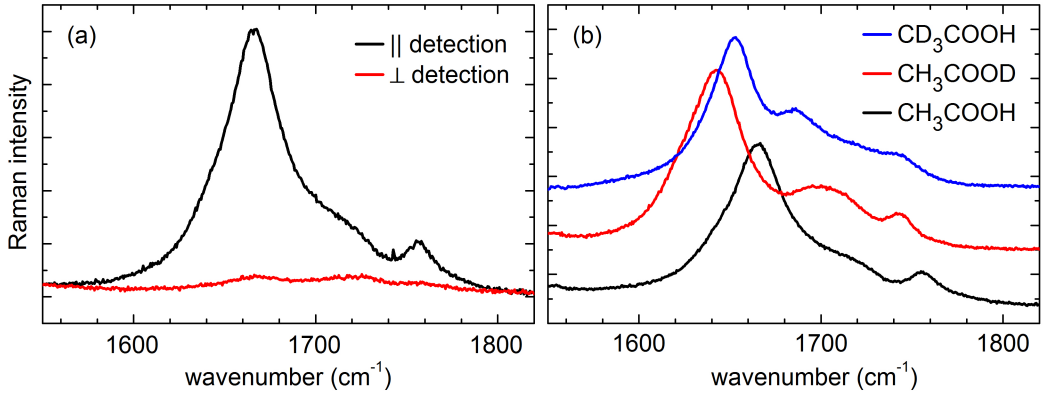

Fig. S4 (a) Raman spectra of neat AA with parallel and perpendicular polarized detection with respect to the excitation polarization. (b) Raman spectra of CH_3COOH, CH_3COOD and CD_3COOH.

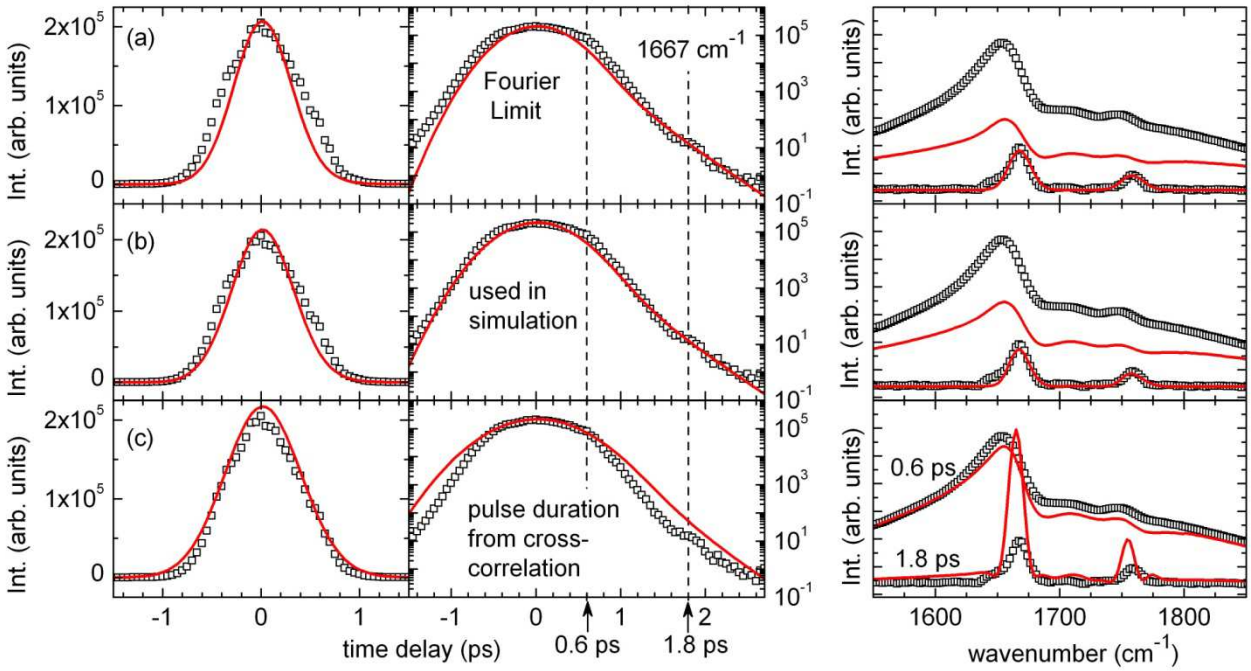

Fig. S5 Simulations of the CARS spectra of neat AA with different pulse lengths. (a) Simulation with a Fouier limited Probe pulse (0.68 ps), (b) with the pulse length used in the simulation (0.73 ps) and (c) with a pulse length attenuated to match with the full width half maximum of the non resonant signal (0.90 ps).

3 Effect of the probe pulse length on the simulations of the CARS spectra

Figure S5 shows simulations of the time and frequency resolved CARS spectra of neat AA for varying probe pulse durations. In panel (a) the pulse duration of a Fourier limited pulse is used with a duration of 0.68 ps calculated from the measured probe pulse spectrum. The amplitudes of the vibrational contributions were adjusted in the simulation while the dephasing times are kept constant. The logarithmic scaled time trace as well as an exemplary spectrum after the cross-correlation show that for the two slowly dephasing contributions good agreement between simulations and data can be achieved. For comparison we show in the next row the simulation with a slightly longer pulse duration of 0.73 ps, which is used in the article. The improvement is that in the falling edge of the cross-correlation a better agreement can be achieved, although the mismatch at a delay of 0.6 ps is still quite large. The last row shows the simulation for a probe pulse duration fitted to the full width half maximum of the time dependent signal far away from resonances. In this spectral region the signal is equal to a cross-correlation measurement, so the time trace reflects the temporal behavior of the probe pulse. Without changing the amplitudes in comparison to the simulation shown in the panel (b) good agreement is seen for short delay times e.g. like in the spectrum in (c) at 0.6 ps. However, it results in an overestimation of the signal at later times which cannot be balanced by amplitude adjustment. In conclusion for the current setup, a simulation with pulse durations calculated from the spectrum or little longer than that leads to the best and most convincing signal reproduction.

4 Accuracy of time resolved CARS with picosecond probe

Due to the sensitivity of the presented CARS spectra to the pulse properties the question arises, which spectral information can be recovered reliable? To elucidate this we use the data of neat AA acid and discuss the dependence of the dephasing parameters on the chosen simulation scenario. Figure S6 shows the integrated signal of the main spectral feature at 1668 cm^{-1} compared to different simulations.

(i) First we show the time behaviour of the signal caused only by the fast dephasing mode (dashed line) with a FWHM of 53 cm^{-1} as used in the article to intimate the reader, how much is left from the measured signal, which has to be modelled by the slowly dephasing mode. Already at a delay time of 1.5 ps the contribution from that mode is by at least a factor of 10 lower than the remaining intensity. This difference increases quickly with delay time. This shows that determining the decay constant of the slowly dephasing mode by fitting a mono exponential single contribution to data at late times, as it is presented in section 3.1, reveals reliable values within the accuracy of the measurement.

(ii) We show the signal simulation of the main feature for a single resonance with a FWHM revealed from the Raman spectrum (black line). By adjusting the amplitudes of the contributions a match to the signal can be obtained during the cross-correlation. However, at late delays this mode cannot recover the signal correctly.

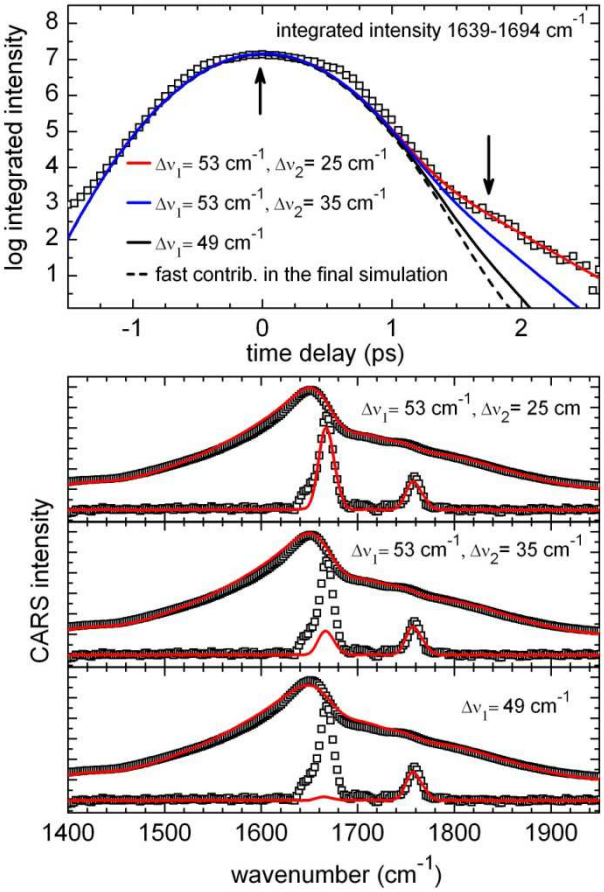

Fig. S6 Integrated time dependent CARS Signal compared with simulations for different dephasing conditions. The amplitudes in all cases are varied to match the signal within the cross-correlation.

(iii) Assuming a combination of modes with widths of 35 cm^{-1} and 53 cm^{-1} (factor 1.5 between the line widths) and attenuating the amplitudes to match the signal at $t_D = 0$ shows also quite large deviations to the signal at late delays and is clearly distinguishable from the measured data. Since this combination already gives a quite large mismatch with the signal we have to conclude, that slower dephasing transitions should be seen with even larger significance. This demonstrates that we can clearly separate two overlapping modes with line widths deviating by a factor of 2.

The parameter for the fast dephasing mode is quite arbitrary regarding only the CARS measurement. In the time resolved CARS this fast mode modulates the spectra only during the cross-correlation. Basically the mode has to be included to describe the spontaneous Raman spectrum consistently, but also from the CARS data strong evidence for this mode can be found. Therefore it is worth to look at the CARS signal without the fast contribution. Since the dephasing constant of the slow mode is pinned down by the signal at late delays, only the nonresonant background and the other two vibrational contributions can be varied to achieve the best possible agreement with the signal during the cross-correlation. Figure S7 shows an optimized

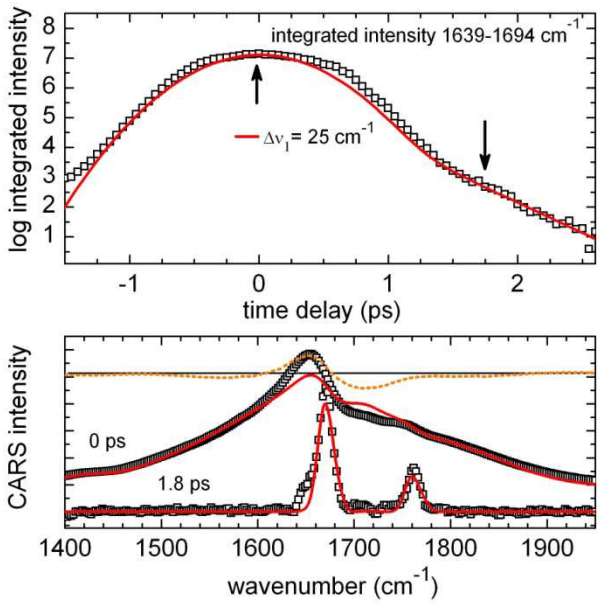

Fig. S7 Integrated time dependent CARS Signal compared with simulations without the fast component. The parameters are optimized to obtain a good match during the cross-correlation without losing the agreement between data and simulation at late delays.

simulation without the fast component. The simulation at late delays agrees nicely with the signal. Within the pulse overlap a systematic deviation can be observed. This deviation might not be as serious as in the spontaneous Raman spectrum, especially if we keep in mind the non ideal probe pulse shape. But the shape of the deviation can be plausibly explained with an additional contribution. In general the emitted field of a resonant contribution is 90° phase shifted with respect to the nonresonant background field at time zero and at the centre transition frequency. Due to the homodyne measurement of the interfering signals an asymmetric, Fano-like spectral shape results. On the red wing of the transition constructive interference is observed and on the blue side intensity is cancelled by destructive interference. The residual of the simulation shows exactly this behaviour, indicating the missing vibrational contribution (see dotted line in Fig. S7).

The line widths for the broad transitions have to be revealed from other experiments. Definitely the spontaneous Raman spectrum, has to be modelled with the incorporated slowly dephasing contributions revealed from the time resolved CARS. If the decay seen in the CARS is mono exponential the shape of these contributions in the Raman spectrum is Lorentzian.